JACS
JOURNAL OF THE AMERICAN CHEMICAL SOCIETY
Communication
pubs.acs.org/JACS

A Mononuclear Manganese(II) Complex Demonstrates a Strategy To Simultaneously Image and Treat Oxidative Stress

Meng Yu,[†] Stephen L. Ambrose,[†] Zachary L. Whaley,[†] Sanjun Fan,[†] John D. Gorden,[†] Ronald J. Beyers,[‡] Dean D. Schwartz,[§] and Christian R. Goldsmith*[,†]

[†]Department of Chemistry and Biochemistry, [‡]Magnetic Resonance Imaging Research Center, and [§]Department of Anatomy, Physiology, and Pharmacology, College of Veterinary Medicine, Auburn University, Auburn, Alabama 36849, United States

Supporting Information

ABSTRACT: A manganese(II) complex with a ligand containing an oxidizable quinol group serves as a turn-on sensor for H_2O_2. Upon oxidation, the relaxivity of the complex in buffered water increases by 0.8 mM^{-1} s^{-1}, providing a signal that can be detected and quantified by magnetic resonance imaging. The complex also serves as a potent antioxidant, suggesting that this and related complexes have the potential to concurrently visualize and alleviate oxidative stress.

The overproduction of reactive oxygen species (ROSs), such as H_2O_2, O_2^-, and hydroxyl radicals, has been associated with several lethal and debilitating health conditions. Heightened oxidative damage to proteins and other biomolecules has been observed in the biopsies and post-mortem examinations of patients suffering from a wide variety of cardiovascular and neurological diseases.[1−4] Understanding the roles that ROSs play in the progressions of these and other conditions requires probes that can monitor their production and traffic within biological systems. Currently, most sensors capable of directly detecting ROSs rely on either fluorescent or luminescent outputs.[5−9] Although these probes provide high spatial resolution, the short wavelengths of light needed to excite the reporter make imaging activity in samples other than thin tissues and cell cultures difficult.

Magnetic resonance imaging (MRI), conversely, uses radio frequency photons to excite the hydrogen nuclei in water molecules and is commonly used to visualize tissues and organs deep within thicker biological samples. Most small molecule MRI contrast agents shorten the longitudinal relaxation times (T_1) of excited protons, allowing sharper contrast between regions with high and low water contents. The ability to accelerate these relaxations defines the relaxivity (r_1) of the contrast agent. A molecule that displays a different r_1 value upon the addition of an analyte can serve as a sensor when monitored by MRI. Several such MRI contrast agent sensors have been developed,[10−12] but few have been directed toward imaging oxidative activity.[13−18] The probes capable of detecting oxidants often either require a co-analyte[13] or display a similar response to O_2[14] or another analyte.[18] Recently, our research group reported a mononuclear manganese complex capable of directly detecting H_2O_2; notably, the complex lacks a chemical response to O_2.[16] Upon oxidation, the mononuclear complexes irreversibly couple into binuclear Mn(II) species. The reaction with H_2O_2 decreases the relaxivity per manganese ion; that the response is a reduction in contrast enhancement limits the probe's ability to resolve different levels of H_2O_2. In the current work, we report a novel manganese-containing MRI contrast agent that responds to H_2O_2 with an altogether different molecular mechanism that results in an increase in the r_1. As with our prior sensor, the oxidation is directed to the organic portion. This differs from a complex recently reported by Caravan's group in which the manganese reporter toggles between the +2 and +3 oxidation states, depending on the local redox environment; due to the lessened paramagnetism, this sensor has a turn-off response to biologically relevant oxidants.[17]

For the organic component of the sensor, we synthesized the hexadentate ligand *N*-(2,5-dihydroxybenzyl)-*N*,*N*′,*N*′-tris(2-pyridinylmethyl)-1,2-ethanediamine (H_2qtp1, Scheme 1). The

Scheme 1

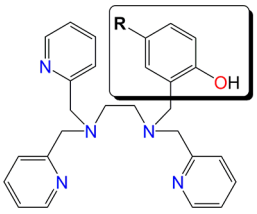

R = OH, H_2qtp1
R = CH_3, Hptp1

$[Mn(H_2qtp1)(MeCN)]^{2+}$ (**1**)
$[Mn(Hptp1)(MeCN)]^{2+}$ (**2**)

H_2qtp1 ligand is prepared in one step from a reaction between the readily synthesized *N*,*N*,*N*′-tris(2-pyridinyl-methyl)-1,2-ethanediamine[19] and commercially available 2,5-dihydroxybenzaldehyde. Pure H_2qtp1 can be obtained through precipitation of the crude from methanol/ether (40% yield).

At first glance, H_2qtp1 strongly resembles the Hptp1 ligand used for our prior sensor; the latter molecule has a methyl group installed *para* to the phenol hydroxyl group.[16] The substitution of a hydroxyl group for the methyl, however, enables a fundamentally different chemical response to oxidants. The redox-active portion of H_2qtp1 is a quinol, which is anticipated to oxidize to a more weakly metal-coordinating *p*-quinone upon exposure to H_2O_2 (Scheme 2) instead of oxidatively coupling to other phenols like Hptp1.[16] Although manganese was not previously known to catalyze quinol oxidation, other redox-active transition metal ions have been reported to do so.[20,21] The manganese therefore serves as both the paramagnetic reporter

Received: July 11, 2014
Published: August 28, 2014

   dx.doi.org/10.1021/ja507034d | *J. Am. Chem. Soc.* 2014, 136, 12836−12839

Scheme 2

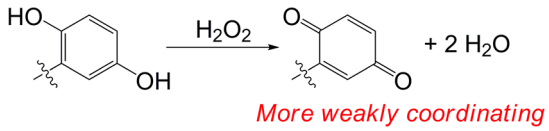

for the contrast agent and the catalyst for the oxidation of the quinol portion of the ligand.

The reaction between H_2qtp1 and manganese(II) triflate in anaerobic acetonitrile yields $[Mn(H_2qtp1)(MeCN)](OTf)_2$ (**1**, MeCN = acetonitrile, OTf^- = triflate). In a typical workup, the complex is crystallized from MeCN/Et_2O mixtures in 82% yield. The crystal structure of **1** reveals that the manganese center is heptacoordinate, with six donor atoms from the H_2qtp1 ligand and one from the coordinated MeCN (Figure 1). The overall

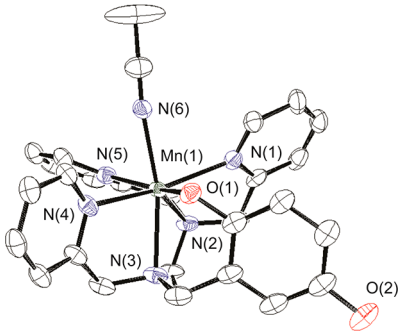

Figure 1. Structure of $[Mn(H_2qtp1)(MeCN)]^{2+}$. All hydrogen atoms and both triflate counteranions are omitted for clarity. All thermal ellipsoids are drawn at 50% probability. Further details about the structure are provided in the Supporting Information.

geometry is best described as a distorted face-capped octahedron, with the quinol O-donor and the three pyridine rings' N-donors defining a pseudoplane. The heptacoordination and the metal–ligand bond distances are both consistent with a +2 oxidation state for the manganese. This assignment is supported by the lack of charge-transfer bands in the optical spectrum and the 5.6 μ_B magnetic moment measured for the solid. The bound quinol remains fully protonated, as evidenced by the anion count and the Mn–O and C–O bond lengths. The C–O bond distances are both 1.38 Å, closely matching those found for quinols encapsulated in clathrates.[22] Each hydroxyl group on the hydroquinone is in close proximity to an O atom from a OTf^- anion; the O–O distances (2.66 Å for O1, 2.71 Å for O2) are consistent with hydrogen-bonding interactions.

Complex **1** is sufficiently stable in aerobic water solutions to allow MRI measurements. The H_2qtp1 ligand does not dissociate from Mn(II) to a noticeable degree, as assessed by the lack of ^{1}H NMR resonances in solutions of **1** in D_2O. The log K for the complexation of H_2qtp1 to Mn(II) was estimated through a titration with the metal-scavenging agent TPEN (*N*,*N*,*N*′,*N*′-tetrakis(2-pyridinylmethyl)ethylenediamine, log K = 10.3).[21] The log K of 10.7 is nearly identical to the 10.6 value estimated for the Hptp1 ligand (Hptp1 = *N*-(2-hydroxy-5-methylbenzyl)-*N*,*N*′,*N*′-tris(2-pyridinylmethyl)-1,2-ethanediamine).[16] Solutions of **1** in H_2O or MeCN are slightly sensitive toward oxygen, with the solutions slowly discoloring from light yellow to purple over 12 h. Over this time, the collected UV/vis spectra display changes in the region between 200 and 300 nm which are consistent with the oxidation of the quinol to a *p*-quinone.[21] Past 24 h, the solution begins to turn brown, consistent with oxidation of the manganese to Mn(III) and/or Mn(IV).

The reactivity between **1** and H_2O_2, conversely, is rapid. In MeCN, the reaction between **1** and excess H_2O_2 turns purple within a few minutes. The corresponding mass spectrum shows new m/z peaks at 454.22 and 657.10, which correspond to the oxidized form of the ligand (qtp1) and its manganese complex with a triflate anion, respectively. The IR spectrum of the solid isolated from the reaction has an intense new absorption at 1658 cm^{-1}, the energy of which is consistent with a carbonyl stretch for a non-metal-coordinated *p*-quinone.[23,24] The reactivity is faster in methanol and water, with the spectroscopic changes occurring in seconds, rather than minutes.

EPR and UV/vis spectroscopy demonstrate that the oxidation state of manganese does not change after adding H_2O_2. The EPR spectra of **1** and its oxidized product are highly similar, with features consistent with high-spin Mn(II). The EPR signal intensity of the Mn(II) in the oxidized product is actually slightly greater than that of an identical concentration of **1**. Upon oxidation, no distinct features are observed in the 350–500 nm region where Mn(III)-related LMCT bands are normally observed.[25,26] The lack of ligand resonance peaks in the NMR of **1** oxidized in D_2O suggests that the oxidized ligand remains bound to the Mn(II) after the reaction.

Analysis of the oxidized product by ^{1}H NMR indicates that the ligand does not oxidize to completion, even with excess H_2O_2. Although both **1** and its oxidized product are NMR-silent, the addition of $Zn(ClO_4)_2$ to solutions of **1** and its oxidized product leads to rapid metal ion exchange, allowing the visualization of diamagnetic Zn(II)-H_2qpt1 and Zn(II)-qtp1 adducts. Using HQ-COSY spectroscopy, we were able to assign two singlet peaks at 6.56 and 7.09 ppm to the hydroxyl protons of H_2qtp1. Upon oxidation, these peaks decrease in intensity by ∼45% but do not vanish completely, as would be anticipated from the complete oxidation of the ligand in the sample. The decrease in these features is invariant and seemingly not correlated to the amount of H_2O_2 added past a stoichiometric amount. Consequently, we currently believe that the oxidation is reversible and that the mixture of qtp1 and H_2qtp1 corresponds to an equilibrium position.

The relaxivity of complex **1** in an aqueous solution of 50 mM HEPES buffered to pH 7.00 was found to be 4.73 mM^{-1} s^{-1} (3 T field, 25 °C). This r_1 value is higher than both the 4.39 mM^{-1} s^{-1} value for the Mn(II) complex with the related Hptp1 ligand and the 1.73 mM^{-1} s^{-1} value for $[Mn(EDTA)(H_2O)]^{2-}$ measured under identical conditions.[16,27] The enhanced relaxivity of **1** relative to $[Mn(Hptp1)(MeCN)](ClO_4)_2$ (**2**) may be due to additional interactions with outer-sphere water molecules made possible by the presence of the second hydroxyl group on the quinol.

Upon the addition of 10 mM H_2O_2, the relaxivity per manganese increases from 4.73 to 5.30 mM^{-1} s^{-1}. Although the change is modest, this represents the first instance of a turn-on response by a mononuclear MRI contrast agent to H_2O_2. We attribute the increase of the relaxivity to the oxidation of the hydroquinone moiety to more weakly coordinating *p*-benzoquinone. In aqueous solution, water molecules should more readily displace the quinone portion of the ligand, resulting in a transiently greater aquation number, which in turn would increase the r_1.[28] This is difficult to ascertain experimentally, given that the sensor is only partially oxidized. The incomplete oxidation also is partly responsible for the modest r_1 response.

dx.doi.org/10.1021/ja507034d | J. Am. Chem. Soc. 2014, 136, 12836–12839

That the same amount of ligand oxidation is observed, even with exceedingly high concentrations of H_2O_2, may suggest that the Mn(II)-qtp1 adduct formed upon oxidation may react with a second equivalent of ROS to return to the reduced state, analogous to a superoxide dismutase (SOD) or catalase enzyme. Evidence does suggest that **1** can catalytically degrade ROSs and behave as an antioxidant (*vida infra*). Complex **1** can be fully oxidized by 2,3-dichloro-5,6-dicyano-1,4-benzoquinone (DDQ). The addition of 1 equiv of DDQ to a solution of **1** is sufficient to completely oxidize the quinol portion of H_2qtp1 to the quinone, as assessed by ^{1}H NMR. In the absence of Zn(II), the DDQ-oxidized product is NMR-silent, suggesting that the oxidized ligand remains bound to the Mn(II). The r_1 value for the fully oxidized sensor is 5.56 mM^{-1} s^{-1}. The addition of 2 mM KO_2 to **1** likewise triggers a stronger response (r_1 = 5.52 mM^{-1} s^{-1}). The chemical change responsible for the MRI response, however, is not identical to those in the H_2O_2 and DDQ experiments, as confirmed by UV/vis and MS analysis of the reaction. The addition of 10 mM NaClO to solutions of **1**, conversely, does not trigger any changes in the spectroscopic features, and the r_1 value (4.82 mM^{-1} s^{-1}) remains essentially equal to that of non-oxidized **1**. The relaxivity results suggest that an excess of H_2O_2 oxidizes ~70% of the sensor in water.

There is limited evidence that the oxidation of the sensor can be reversed by reductants. The addition of sodium dithionite to a H_2O_2-oxidized solution of **1** in MeOH changes the color from purple to light yellow; the UV/vis spectrum, however, has a much more intense band around 300 nm, which suggests the formation of a different coordination compound. Further analysis suggests that the ligand's oxidation has been reversed. The IR spectrum of the product lacks the 1658 cm^{-1} feature indicative of the quinone, and the organic isolated from the reaction mixture appears to be entirely H_2qtp1 on the basis of its ^{1}H NMR spectrum.

Cyclic voltammetry (CV) of **1** in an aqueous solution of phosphate buffered to pH 7.2 reveals two redox features. The lower potential of the two has an $E_{1/2}$ of 115 mV vs Ag/AgCl and is highly reversible (ΔE = 75 mV). Since a comparable redox process is observed in the CV of a Zn(II)-H_2qtp1 adduct, this feature can be firmly assigned to the oxidation and reduction of the H_2qtp1 ligand. This potential translates to 310 vs NHE, which is both comparable to the M(III)/M(II) reduction potentials of iron and manganese SODs[29] and within error of the 300 mV value that is generally accepted to be ideal for the dismutation of O_2^{-}.[30,31] The higher potential feature at 680 mV vs Ag/AgCl (880 mV vs NHE) is irreversible. Since an analogous feature is not observed with the zinc analog, we have assigned this to the oxidation of Mn(II) to Mn(III).

As anticipated from the electrochemistry, **1** behaves as a potent SOD mimic (Figure 2). The previously prepared **2** was also tested for this activity. The SOD mimicry was assessed using an established procedure that uses xanthine oxidase to produce O_2^{-}.[32,33] Both Mn(II) compounds are extremely effective at degrading O_2^{-}, with IC_{50} values of 11.3 nM (**1**) and 7.7 nM (**2**). These values compare well with those of the best reported mimics for SOD, which are all manganese complexes with electronically modified porphyrin ligands.[32]

The antioxidant properties of **1** and **2** were also assessed using the DPPH assay (DPPH = 2,2-diphenyl-1-picrylhydrazyl radical hydrate), which evaluates the ability of a compound to donate hydrogen atoms to DPPH to yield the corresponding hydrazine.[34−36] Although **1** and **2** are similar with respect to their abilities to intercept O_2^{-} prior to its reaction with lucigenin,

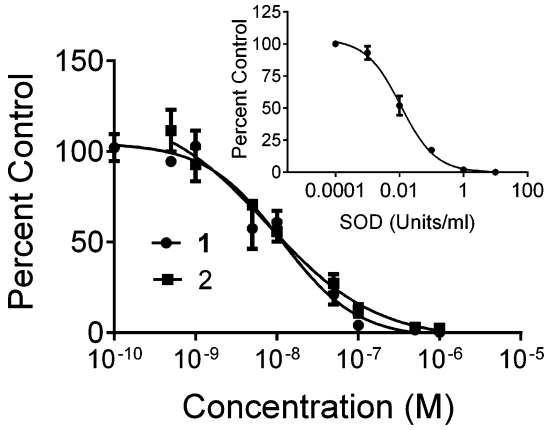

Figure 2. Superoxide scavenging effects of **1** and **2**. Superoxide was generated using a hypoxanthine−xanthine oxidase reaction and detected using the chemiluminescent probe lucigenin. Reactions were carried out in 50 mM Tris-HCl (pH 8.0) containing either **1**, **2**, or Cu/Zn SOD from bovine erythrocytes (inset). Data for the various concentrations of **1**, **2**, and SOD are expressed as a percentage of luminescence in the presence of vehicle.

the DPPH assay suggests that **1** is the superior antioxidant (Figure 3). The IC_{50} value for **1** was found to be 6.6 μM; by this

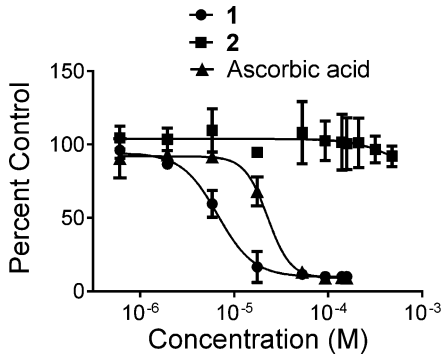

Figure 3. DPPH free radical scavenging assay of **1**, **2**, and ascorbic acid. The antioxidants were added to DPPH and incubated in the dark for 30 min at room temperature. Spectroscopic measurements were performed at 517 nm. The data were normalized to the absorbance in the presence of vehicle. All experiments were performed in triplicate and repeated twice.

measure, it bests the well-known antioxidant ascorbic acid (IC_{50} = 22.3 μM). The Hptp1 complex, conversely, fails to reduce DPPH to a noticeable degree.

One concern that has limited the application of redox-active metals in biological imaging is that they can elevate ROS concentrations. The results here demonstrate that the opposite can be true and that there exists the potential to simultaneously image and mitigate the oxidative stress caused by aberrantly high concentrations of ROSs. The cytotoxicities of **1** and **2** have been assessed with H9c2 cells. The cells can tolerate 10 μM doses of both compounds for 4 h and a 1.0 μM dose of **1** for 24 h. Higher dosages and/or longer incubation times do trigger noticeable cell death.

We attempted to see if **1** could be used to detect and treat oxidative stress in RAW264.7 mouse macrophage and H9C2 rat cardiac cells. Regrettably, the probe does not appear to enter either type of cell. The T_1 values of cells that were treated with **1**, rinsed, then suspended in Hanks Balanced Salt Solution (HBSS)

dx.doi.org/10.1021/ja507034d | J. Am. Chem. Soc. 2014, 136, 12836−12839

were within error of those for cells that had not been exposed to the probe. EPR analysis of the rinses confirmed that most of the sensor remained in the extracellular fluid. We then attempted to use **1** to detect oxidative stress in the extracellular fluid, but the addition of 200 μM H_2O_2 did not increase the T_1 values of H9C2 cells that were suspended in HBSS containing 100 μM **1**. The results suggest that the sensor will need to be further stabilized and rendered cell permeant before successful *in vivo* imaging or treatment of oxidative stress can be accomplished.

In summary, we have synthesized a MRI contrast agent that uses a redox-active ligand to signal the presence of H_2O_2. Unlike our prior sensor, the ligand oxidation appears to be reversible, which may allow related sensors to distinguish highly oxidizing regions within biological samples. We speculate that the ligand oxidation results in a more weakly coordinating ligand, and that the increase in r_1 results from greater aquation of the manganese. Although the relaxivity change is modest, the results demonstrate the feasibility of this strategy for H_2O_2 detection. Additionally, the H_2qtp1 complex is a potent antioxidant, as assessed by two common assays for such activity. Related compounds may therefore be able to serve as theranostic agents for oxidative stress.

■ ASSOCIATED CONTENT

Ⓢ Supporting Information

Experimental details, analysis of iron-for-manganese exchange from **1**, spectroscopic analyses of the reaction between **1** and H_2O_2, structural data for **1**, r_1 measurements showing MRI response of **1** to H_2O_2 and other oxidants, CV of **1** and its Zn(II) analogue, and cytotoxicity studies with H9c2 cells. This material is available free of charge via the Internet at http://pubs.acs.org.

■ AUTHOR INFORMATION

Corresponding Author

crgoldsmith@auburn.edu

Notes

The authors declare no competing financial interest.

■ ACKNOWLEDGMENTS

The authors are grateful to Prof. Evert Duin for his help with obtaining and analyzing EPR data. We also thank Prof. Curtis Shannon and Ms. Cristine Kreitzer for technical assistance. We thank Auburn University, the Auburn University MRI Research Center, and the American Chemical Society, donors of the Petroleum Research Fund (Grant 49532-DNI3), for financial support. A NSF EPSCoR/AU-CMB summer fellowship provided additional support to M.Y.

■ REFERENCES

(1) Dexter, D. T.; Carter, C. J.; Wells, F. R.; Javoy-Agid, F.; Agid, Y.; Lees, A.; Jenner, P.; Marsden, C. D. *J. Neurochem.* **1989**, *52*, 381−389.
(2) Viappiani, S.; Schulz, R. *Am. J. Physiol. Heart Circ. Physiol.* **2006**, *290*, H2167−H2168.
(3) Shishehbor, M. H.; Aviles, R. J.; Brennan, M.-L.; Fu, X.; Goormastic, M.; Pearce, G. L.; Gokce, N.; Keaney, J. F., Jr.; Penn, M. S.; Sprecher, D. L.; Vita, J. A.; Hazen, S. L. *J. Am. Med. Assoc.* **2003**, *289*, 1675−1680.
(4) Askenov, M. Y.; Askenova, M. V.; Butterfield, D. A.; Geddes, J. W.; Markesbery, W. R. *Neuroscience* **2001**, *103*, 373−383.
(5) Lippert, A. R.; Van de Bittner, G. C.; Chang, C. J. *Acc. Chem. Res.* **2011**, *44*, 793−804.
(6) Maeda, H.; Yamamoto, K.; Nomura, Y.; Kohno, I.; Hafsi, L.; Ueda, N.; Yoshida, S.; Fukuda, M.; Fukuyasu, Y.; Yamauchi, Y.; Itoh, N. *J. Am. Chem. Soc.* **2005**, *127*, 68−69.
(7) Koide, Y.; Urano, Y.; Kenmoku, S.; Kojima, H.; Nagano, T. *J. Am. Chem. Soc.* **2007**, *129*, 10324−10325.
(8) Soh, N. *Anal. Bioanal. Chem.* **2006**, *386*, 532−543.
(9) Chen, X.; Tian, X.; Shin, I.; Yoon, J. *Chem. Soc. Rev.* **2011**, *40*, 4783−4804.
(10) Caravan, P. *Acc. Chem. Res.* **2009**, *42*, 851−862.
(11) Esqueda, A. C.; López, J. A.; Andreu-de-Riquer, G.; Alvarado-Monzón, J. C.; Ratnakar, J.; Lubag, A. J. M.; Sherry, A. D.; De León-Rodríguez, L. M. *J. Am. Chem. Soc.* **2009**, *131*, 11387−11391.
(12) Major, J. L.; Parigi, G.; Luchinat, C.; Meade, T. J. *Proc. Natl. Acad. Sci. U.S.A.* **2007**, *104*, 13881−13886.
(13) Chen, J. W.; Pham, W.; Weissleder, R.; Bogdanov, A., Jr. *Magn. Reson. Med.* **2004**, *52*, 1021−1028.
(14) Raghunand, N.; Jagadish, B.; Trouard, T. P.; Galons, J.-P.; Gillies, R. J.; Mash, E. A. *Magn. Reson. Med.* **2006**, *55*, 1272−1280.
(15) Ratnakar, S. J.; Viswanathan, S.; Kovacs, Z.; Jindal, A. K.; Green, K. N.; Sherry, A. D. *J. Am. Chem. Soc.* **2012**, *134*, 5798−5800.
(16) Yu, M.; Beyers, R. J.; Gorden, J. D.; Cross, J. N.; Goldsmith, C. R. *Inorg. Chem.* **2012**, *51*, 9153−9155.
(17) Loving, G. S.; Mukherjee, S.; Caravan, P. *J. Am. Chem. Soc.* **2013**, *135*, 4620−4623.
(18) Viger, M. L.; Sankaranarayanan, J.; de Gracia Lux, C.; Chan, M.; Almutairi, A. *J. Am. Chem. Soc.* **2013**, *135*, 7847−7850.
(19) Mialane, P.; Nivorojkine, A.; Pratviel, G.; Azéma, L.; Slany, M.; Godde, F.; Simaan, A.; Banse, F.; Kargar-Grisel, T.; Bouchoux, G.; Sainton, J.; Horner, O.; Guilhem, J.; Tchertanova, L.; Meunier, B.; Girerd, J.-J. *Inorg. Chem.* **1999**, *38*, 1085−1092.
(20) Maurya, M. R.; Sikarwar, S. *J. Mol. Catal. A* **2007**, *263*, 175−185.
(21) Owsik, I.; Kolarz, B. *J. Mol. Catal. A* **2002**, *178*, 63−71.
(22) Chan, T.-L.; Mak, T. C. W. *J. Chem. Soc., Perkin Trans. 2* **1983**, 777−781.
(23) Glick, M. D.; Dahl, L. F. *J. Organomet. Chem.* **1965**, *3*, 200−221.
(24) Meyerson, M. L. *Spectrochim. Acta, Part A* **1985**, *41*, 1263−1267.
(25) Goldsmith, C. R.; Cole, A. P.; Stack, T. D. P. *J. Am. Chem. Soc.* **2005**, *127*, 9904−9912.
(26) Hubin, T. J.; McCormick, J. M.; Alcock, N. W.; Busch, D. H. *Inorg. Chem.* **2001**, *40*, 435−444.
(27) Zhang, Q.; Gorden, J. D.; Beyers, R. J.; Goldsmith, C. R. *Inorg. Chem.* **2011**, *50*, 9365−9373.
(28) Caravan, P.; Ellison, J. J.; McMurry, T. J.; Lauffer, R. B. *Chem. Rev.* **1999**, *99*, 2293−2352.
(29) Miller, A.-F. *Acc. Chem. Res.* **2008**, *41*, 501−510.
(30) Batinic-Haberle, I.; Rajic, Z.; Tovmasyan, A.; Reboucas, J. S.; Ye, X.; Leong, K. W.; Dewhirst, M. W.; Vujaskovic, Z.; Benov, L.; Spasojevic, I. *Free Radical Biol. Med.* **2011**, *51*, 1035−1053.
(31) Aitken, J. B.; Shearer, E. L.; Giles, N. M.; Lai, B.; Vogt, S.; Reboucas, J. S.; Batinic-Haberle, I.; Lay, P. A.; Giles, G. I. *Inorg. Chem.* **2013**, *52*, 4121−4123.
(32) Iranzo, O. *Bioorg. Chem.* **2011**, *39*, 73−87.
(33) McCord, J. M.; Fridovich, I. *J. Biol. Chem.* **1969**, *244*, 6049−6055.
(34) Kedare, S. B.; Singh, R. P. *J. Food Sci. Technol.* **2011**, *48*, 412−422.
(35) Blois, M. S. *Nature* **1958**, *181*, 1199−1200.
(36) Milaeva, E. R.; Shpakovsky, D. B.; Gracheva, Y. A.; Orlova, S. I.; Maduar, V. V.; Tarasevich, B. N.; Meleshonkova, N. N.; Dubova, L. G.; Shevtsova, E. F. *Dalton Trans.* **2013**, *42*, 6817−6828.